Chemical Engineering Journal 347 (2018) 74–83

Contents lists available at ScienceDirect

Chemical Engineering Journal

journal homepage: www.elsevier.com/locate/cej

Biotransformation of cadmium-sulfamethazine combined pollutant in aqueous environments: *Phanerochaete chrysosporium* bring cautious optimism

Xueying Guo[a,c,1], Zhiwei Peng[b,c,1], Danlian Huang[a,c,*], Piao Xu[a,c], Guangming Zeng[a,c,*], Shuang Zhou[a,c], Xiaomin Gong[a,c], Min Cheng[a,c], Rui Deng[a,c], Huan Yi[a,c], Hao Luo[a,c], Xuelei Yan[a,c], Tao Li[a,c]

[a] College of Environmental Science and Engineering, Hunan University, Changsha 410082, China
[b] Zoomlion Heavy Industry Science and Technology Co., Ltd, Changsha 410013, China
[c] Key Laboratory of Environmental Biology and Pollution Control (Hunan University), Ministry of Education, Changsha 410082, China

HIGHLIGHTS

- The co-contamination can be efficiently removed by *Phanerochaete chrysosporium*.
- Complex mode of Cd and sulfamethazin was distinctly different at different pH.
- Antioxidant in fungi cell was higher than that induced by individual pollutant.
- Biotransformation efficiency can be enhanced with the concentration ratio changed.

GRAPHICAL ABSTRACT

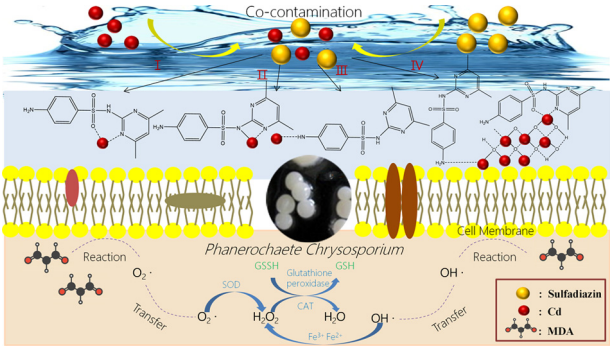

ARTICLE INFO

Keywords:
Cadmium
Sulfamethazine
Co-contamination
Biotransformation
Resistance
Phanerochaete chrysosporium

ABSTRACT

Microorganism biotransformation of sulfamethazine (SMT) in aqueous environments is a major concern, especially considering their exposure to coexisting SMT and heavy metals. *Phanerochaete chrysosporium* (*P. chrysosporium*) is a more concerned Cadmium (Cd) and SMT hyper accumulation specie. This study, referring to metabolic mechanisms and application, was performed to investigate the single and combined effects of Cd-SMT, including toxicity, resistance, as well as the accumulation and biotransformation by *P. chrysosporium*. The results revealed that Cd-SMT co-contamination caused increasing active oxygen accumulation, and the number of antioxidant enzyme and non-enzymatic antioxidants were higher than that under the stress of their individual pollution. It was found that *P. chrysosporium* accumulated high levels of Cd with the increment of 6.98–23.96% induced by Cd-SMT co-contamination compared to under the stress of Cd individual pollution. What's more, the addition of Cd reduced the toxicity of SMT to *P. chrysosporium*. The decrease of malonaldehyde and the increase of protein also proved that *P. chrysosporium* held enormous potential to fit in the co-contaminated environment, and to remediate the co-contaminated water especially in the long-term treatment. These results undoubtedly

* Corresponding authors at: College of Environmental Science and Engineering, Hunan University, Changsha 410082, China.
E-mail addresses: huangdanlian@hnu.edu.cn (D. Huang), zgming@hnu.edu.cn (G. Zeng).
[1] These authors contribute equally to this article.

https://doi.org/10.1016/j.cej.2018.04.089
Received 18 February 2018; Received in revised form 10 April 2018; Accepted 13 April 2018
Available online 16 April 2018
1385-8947/

contribute to the development of fungi-based technologies and the applications of *P. chrysosporium* in realistic environment rather than laboratory simulation environment.

1. Introduction

Sulfonamide antibiotics (SAs) which are widely used by humans and veterinary medicine are of great concerns because of their frequent detections in soils and groundwater. It has been reported that the concentrations of SAs in manure reached 900 mg kg^{-1} [1]. Sulfonamides appear frequently in the effluents of sewage treatment plant with concentrations reported to be 6 μg L^{-1} in Germany, 290 μg L^{-1} in Switzerland, 395–575 μg L^{-1} in Georgia, USA, and 0.06–0.21 μg L^{-1} in Colorado, USA [2–4]. Moreover, evidences showed that the half-life of SAs is 9.6–833 d, therefore the time duration of SAs is too long in the water and sediment of environment and they also pose potential risks to aquatic species, plants and human being [5,6]. Sulfamethazine (SMT), a kind of SAs, is highly hydrophilic (octanol water partition coefficient: SMT log K_{ow} = 0.27) even in neutral form. It shows a good performance in inhibiting the enzymatic reaction in bacteria, via deferring the synthesis of an important coenzyme *para*-aminobenzoic acid and damaging the function of product purines and pyrimidines [7]. Heavy metals (HMs) are another matter of concern for their damage on ecosystem and living organisms [8,9]. Cadmium (Cd) is a highly toxic metal which can easily enrich in food chain and dissolve readily in water by natural processes and anthropogenic activities. It can be easily accumulated in crops, and further cause numerous symptoms and pathologies of animals and humans, such as neurological effects and endocrine dyscrasia [10,11].

Environmental behavior of individual contaminant is a popular topic in laboratory investigation [12–14]. But the research of co-contamination is a more practical issue with the development of industry and the acceleration of urbanization. Therefore, combined pollution has become an important developing direction of environment science. In realistic environment, various pollutants always co-exist and even react with each other to make the environmental pollution diversified and complicated. Therefore, as typical pollutants in the environment, heavy metals-antibiotic combined pollutant, especially Cd-SMT combined pollutant, got popularly attention nowadays.

Data from the literature indicate a greater tolerance of white rot fungi (WRF), which are capable of not only degrading SAs but also immobilizing of HMs via unique extracellular oxidative enzyme systems, cell wall cation exchange, extracellular chelation with organic acids and intracellular bioaccumulation [15,16]. Kim et al. [17] discovered that O-methyltransferases in WRF can accelerate SAs degradation by converting the major inhibitors OH-SAs into non-toxic methylated phenolic ones. Rodríguez et al. [18] made a point that WRF-laccase system can promote the degrading efficiency of SAs to 75%. Li et al. [19] proved that the addition of WRF can increase the Cd removal rate from 44.85 to 80.36%. These findings also signaled that WRF possessed potential ability to biotransform HMs-SAs co-contamination. Their high tolerance protects them from the high-level concentrations of organic pollutants and HMs so that their enzyme system could function normally in harsh environments. *Phanerochaete chrysosporium* (*P. chrysosporium*) is a more concerned Cd-SMT combined pollutant hyper accumulation species of WRF [20,21]. The main removal mechanisms were (i) biosynthesis of phytochelatin (PCs) and metallothioneins (MTs) in cells, (ii) phosphate and polyphosphate metabolisms, (iii) chelate with malate and oxalate, (iv) the functional group added to the reactants by CYP450 monooxygenases, such as hydroxyl, carboxyl, or an amine group, and (v) metabolism product conjugated by non-specific extracellular oxidizing agents such as sulfates, glucuronides, glucosides, and glutathione (GSH) [22].

Toxicity and resistance effects, which produced in the interaction process, are closely related to the biotransformation efficiency of pollutant. Most attention has been paid toward the extracellular enzymes, the generation of reactive oxygen species (ROS) and free radical scavenging capacity. These indicators are more beneficial to assess practicability of one biotechnology and reveal the deep mechanisms in transformation process of xenobiotics. In this study, we not only investigated the biotransformation performance of Cd-SMT combined pollutant by *P. chrysosporium*, but also detected the toxicity and resistance indicator, such as ROS, malonaldehyde (MDA), catalase (CAT), superoxide dismutase (SOD) and polyphenol oxidase (PPO), to uncover the underlying mechanisms induced by HMs and antibiotics. Therefore, the objectives of this study were to provide insight into the biotransformation pathway of combined pollutant and to enhance the application and practical value of biotechnology in real environment.

2. Materials and methods

2.1. Microorganism, chemicals, and media

The fungus *P. chrysosporium* strain ATCC-24725 was obtained from China Center for type Culture Collection (Wuhan, China). Fungal cultures were maintained on potato dextrose agar (PDA) slants at 4 °C, and then transferred to PDA plates at 37 °C for 3 days. The spores on the agar surface were gently scraped and blended in the sterile distilled water as spore suspension. The spore concentration was measured by a microscope with a blood cell counting chamber and adjusted to 2.0×10^6 CFU per mL.

The analytical standard of sulfamethazine (99%, w/w) was purchased from Sigma-Aldrich. Analytical reagent grade $FeSO_4$, $K_3Fe(CN)_6$, Na_2HPO_4 and NaH_2PO_4 were obtained from Sinopharm Chemical Reagent Co., Ltd. China. Tert-butanol (TBA), 2,7-dichlorodihydrofluoresceindiacetate (DCFH-DA), hydroxylammonium chloride, 2,2′-azino-bis(3-ethylbenzothiazoline-6-sulphonic acid) (ABTS), pyrogallic acid (PAPG), 5,5′-Dithiobis-(2-nitrobenzoic acid) (DTNB), trichloroaceti-cacid (TCA), bovine serum albumin (BSA) and sulfanilic acid were purchased from Aladdin Chemistry Co., Ltd. China. Acetonitrile and methanol were of HPLC grade and obtained from Merck KgaA. Ultrapure water (resistivity of 18.2 MΩ cm) was used throughout the experiments.

2.2. Experimental design

Liquid-state conditions were selected to simulate the real aqueous environment. 5.0 mL of aqueous spore suspension of *P. chrysosporium* was inoculated into 250 mL Erlenmeyer flasks containing 100 mL Kirk's liquid culture medium [23] for 3 days. Controlled the final SMT level at 0, 10, 30 and 50 mg L^{-1} (G1), the final Cd level at 0, 10, 50 and 100 mg L^{-1} (G2) and the final Cd-SMT combined pollutant level at 0, 10–30, 50–30, 100–30, 50–10 and 50–50 mg L^{-1} (G3), respectively. 1.0 g *P. chrysosporium* wet biomass was mixed with 50 mL aqueous solution at various initial Cd and SMT concentrations. Finally, the mixture was incubated in a constant temperature incubator with a constant speed of 120 rpm at 30 °C for 72 h. Sampling was performed after 6, 12, 16, 24, 36, 48, 60 and 72 h. The preparation method of cell free extract was shown in Supplementary information (SI) in detail.

2.3. Quantitative analysis by HPLC

The SMT concentration in samples was monitored by an Agilent high-performance liquid chromatography (HPLC) Series 1100 (Agilent,

Waldbronn, Germany) equipped with an auto-sampler and a UV-Vis detector. The UV detector was set at 268 nm and the Zorbax SB-C18 column (4.6 × 250 mm, 5 mm) was used in SMT detection. The column oven temperature was set to 25 °C. The injection volume was 50 μL and the initial eluent flow rate was 1 mL min^{-1}. Mobile phase A was composed of 80% HPLC grade methyl alcohol, and mobile phase B was 20% HPLC grade acetonitrile. All samples were measured twice and the data were averaged for further data processing [24].

2.4. Oxidative stress estimation

To determine the MDA concentration, TBA reaction was used according the method of Dhindsa et al. with slight modifications [25]. An assay for proteins depends on the reaction of Coomassie brilliant blue G250 in dilute acid [26]. The modified TBA method was used to determine ·OH [27]. TBA-reactive substances (TBARS) were used to render the results. The intracellular content of $O_2\cdot^-$ was estimated by measuring the formation of NO_2^- modified by Oracz et al. [28]. The degree of ROS generation was performed by a fluorometric indicator H_2DCF-DA, as previously introduced by Chen et al. [29]. The specific method was detailed in SI. In addition to the traditional methods, the electron spin resonance (ESR) was used to detected the radical species, and DMPO (pH = 7.4, 40 mM phosphate buffer) was used as the spin trap reagent in this study. The EPR spectra was obtained at room temperature by a JES-FA 200 spectrometer (Japan), with a resonance frequency of 9.20 GHz, microwave power of 0.998 mW, modulation frequency of 100 kHz, modulation amplitude of 2.0 G, center field of 3465, sweep width of 100 G, time constant of 30 ms [30].

2.5. Resistance system assessment

Ellman's reagent, containing 0.6 mM DTNB, 5 mM EDTA and 120 mM phosphate buffer solution (PBS), was used to estimate non-protein thiols (NP-SH) by absorbance measurement at 412 nm [31]. Hydroxyl radical scavenging activity was indicated by Smirnoff and Cumbes method [32]. CAT in 0.2 mL intracellular extraction buffer was determined by 2 mL 100 mM PBS (pH = 7.4) at 240 nm, and 0.5 mL of 100 mM H_2O_2 was used as the initiator [33]. SOD activity was determined by quantifying the inhibition of pyrogallol self-oxidation [34]. The specific method was detailed in SI.

2.6. Data analysis

Data were presented as the means of three replicates, and the standard deviations were used to analyze the experimental data. Statistical analyses were performed using the software package SPSS 18.0 (SPSS Inc, Chicago, IL, USA). Data on the toxicity and resistance experiment and removal experiment in *P. chrysosporium* were subjected to one-way analysis of variance (ANOVA) tests, followed by Duncan's test ($p < 0.05$), to determine the significance of the differences between the treatments.

3. Results and discussion

3.1. Reactive oxygen species generation under Cd-SMT stress of P. chrysosporium

ROS is always seen just like an initiator of oxidative stress and the

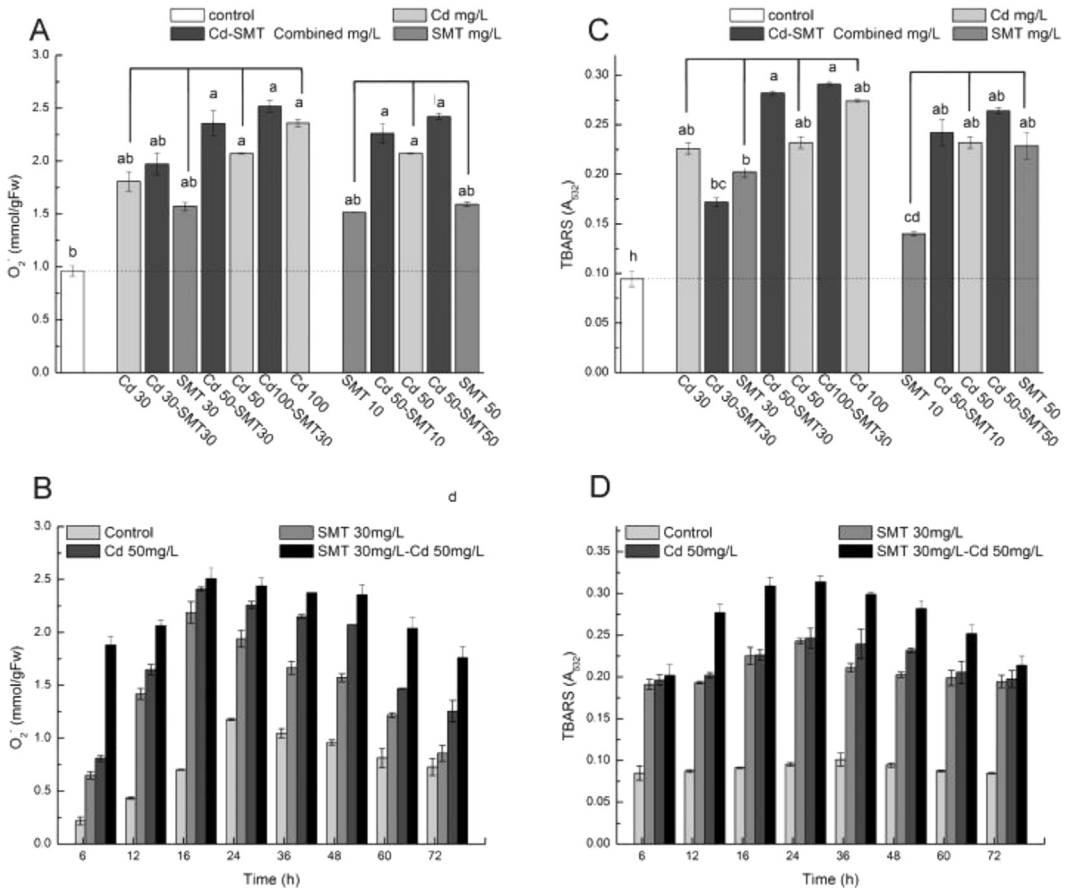

Fig. 1. Concentrations of $O_2\cdot-$ (A) and ·OH (C) exposed to a range of 0–100 mg L^{-1} Cd and 0–50 mg L^{-1} SMT for 48 h, and time-cause of $O_2\cdot-$ (B) and ·OH (D) variation under Cd 50 mg L^{-1}, SMT 30 mg L^{-1} and Cd 50-SMT 30 mg L^{-1} in *P. chrysosporium*. The bars represent the standard deviations of the means (n = 3), and the values followed by different letters in the same figure differ significantly ($p < 0.05$).

most common ones of them are superoxide ($O_2\cdot^-$), the hydroxyl radical (·OH) and hydrogen peroxide (H_2O_2). Heavy metals, in addition to binding to aromatic amino acid residues in enzyme molecules, can cause oxidative damage of proteins by the induction of oxidative stress associated with the production of ROS [35,36]. The productions of free radicals were shown in Fig. 1. It was observed that, at 48 h, G3 (Cd-SMT combined contamination) presented the highest yield of $O_2\cdot^-$. Next to which was G2 (Cd treatment alone) and the lowest production was detected in G1 (SMT treatment alone), as shown in Fig. 1A. Apparently, as the concentration of xenobiotics increased, $O_2\cdot^-$ content increased in all experimental group. The results indicated that: (i) the production of $O_2\cdot^-$ could be stimulated by a higher concentration of xenobiotics, and (ii) Cd-SMT combined pollutant can bring about a higher level of $O_2\cdot^-$ content than their individual contaminant. The concentration of $O_2\cdot^-$ in all groups reached the highest level at 16 h, with the concentration of 2.19, 2.41 and 2.51 mmol g^{-1}, except for the control (Fig. 1B). Then most of them decreased and finally reached the level which was similar to the control. This phenomenon was possibly due to the two steps reaction: (i) in the beginning of the period, veratryl alcohol generated under the stress of xenobiotics was oxidized to cation radical by lignin peroxidase, then the cation radical oxidize oxalate to $CO_2\cdot^-$, and after that $CO_2\cdot^-$ convert O_2 to $O_2\cdot^-$ [37], and (ii) in later stage, the production of SOD was increased in *P. chrysosporium*, which can convert $O_2\cdot^-$ to hydrogen peroxide, so that the concentration of $O_2\cdot^-$ was decreased. What's very interesting is that, after 60 h, the concentration of $O_2\cdot^-$ in *P. chrysosporium* induced by Cd 50-SMT 30 mg L^{-1} combined pollution dropped rapidly and the value was lower than that under the stress of Cd 50 mg L^{-1} and SMT 30 mg L^{-1} individually, which was opposite to the prior phenomenon. The possible reason is that a higher enzyme activity was stimulated by the more virulent combined pollutant. These resistant mechanisms in *P. chrysosporium* may account for the decrease of $O_2\cdot^-$ content. This phenomenon was what we also called the hormesis, which caused by overcompensation effect.

The ·OH with an oxidation potential of 2.8 eV, is the most reactive species among all ROS. It is particularly unstable and will react rapidly and non-specifically with most biological molecules [38]. The concentration of ·OH was evaluated by measuring the absorbance of the extract, and the concentration of free radicals was proportional to the absorbance. Fig. 1C showed the absorbance corresponding to the concentration of ·OH. It was obvious that the productions of ·OH in G3 was a little higher than G1 and G2, and at the same concentration of 30 mg L^{-1} and 50 mg L^{-1}, the absorbance of G2 was higher than that of G1. A majority of them fit the rules that the concentration of ·OH increases with increasing content of xenobiotics, except Cd 50-SMT 30 mg L^{-1} and Cd 50-SMT 50 mg L^{-1}. The concentration of ·OH in the former was higher than that of the latter, with absorbance of 0.182 and 0.164, respectively. As it happens for all systems, the highest concentration of ·OH was observed at 24 h which was a little later than $O_2\cdot^-$ (Fig. 1D). One of the reasons is obvious: A portion of hydrogen peroxide converted by $O_2\cdot^-$ was catalyzed by Fe^{2+} and then generated ·OH. Therefore, the increase of ·OH is often accompanied by the decrease of $O_2\cdot^-$. The following two reasons mainly contributed to the generation and growth of ·OH: (i) Fenton reaction: H_2O_2 is reduced by Fe^{2+} to produce ·OH, and (ii) Haber-Weiss reaction: Fe^{3+} is reduced to Fe^{2+} by $O_2\cdot^-$, and the generated Fe^{2+} possesses the ability to reduce H_2O_2 to ·OH in return [39,40]. The concentration of ·OH decreased after 36 h on account of the intracellular defensive system, that was what we also called hydroxyl radical scavenging activity. And it would be discussed in greater detail in SI.

The ESR is a more direct way to detect the radical species and DMPO is one of the most efficient oxygen-radical spin trap to detect hydroxyl radical because of the high sensitivity and recognition degree [41]. The ESR spectra also indicated some distinct and interesting results. As shown in Fig. 2A, four-line spectrum were formed with an intensity ratio of 1:2:2:1, which were characteristic peak of ·OH radicals adducted to DMPO. The intensity of the 2nd peak can be used for quantification of ·OH production, with g = 2.005, a_N = 14.96 G, a_H = 14.78 G. The intensity of signal represents the concentration of ·OH in *P. chrysosporium*. After 24 h treated, the signal intensity appeared to differ apparently. The intensity of the sample treated by Cd-SMT combined pollutant was the highest one in all group, which was a little higher than that induced by 50 mg L^{-1} Cd and much higher than that treated with 30 mg L^{-1} SMT. This phenomenon indicated that the production of ·OH was easier to stimulated induced by Cd-SMT combined pollutant rather than under the stress of the other individual pollutant, and the yield was higher under the stress of Cd rather than SMT. This phenomenon was consistent with the result detected by TBA, which scrupulously revealed the changes of physiological index and the damage mechanisms induced by xenobiotic.

The generation of total intracellular ROS was qualitatively analyzed by confocal laser scanning microscopy coupled with H_2DCF-DA assay to explore the intracellular oxidative stress of Cd-SMT individual and combined pollution at 24 h. The green fluorescence intensity represents the ROS level of *P. chrysosporium* (Fig. 2B). All samples of experimental groups presented significant differences compared with the control. The fluorescence intensity of Cd-SMT combined pollution was much higher than that under the stress of SMT, and a little higher than that under the stress of Cd. These phenomena further evidence that Cd-SMT combined pollutant can bring about a higher level of ROS than their individual contaminant.

3.2. Antioxidant enzyme activity analysis

Generally, antioxidants, which possess the capacity to terminate the chain reactions of radical and prevent cell damage from oxidative stress, can be divided into two categories: antioxidant enzymes and non-enzymatic antioxidants. In this study, two antioxidant enzymes, SOD and CAT, have been monitored under the different concentration at different time. SOD is a kind of enzyme that catalyze the breakdown

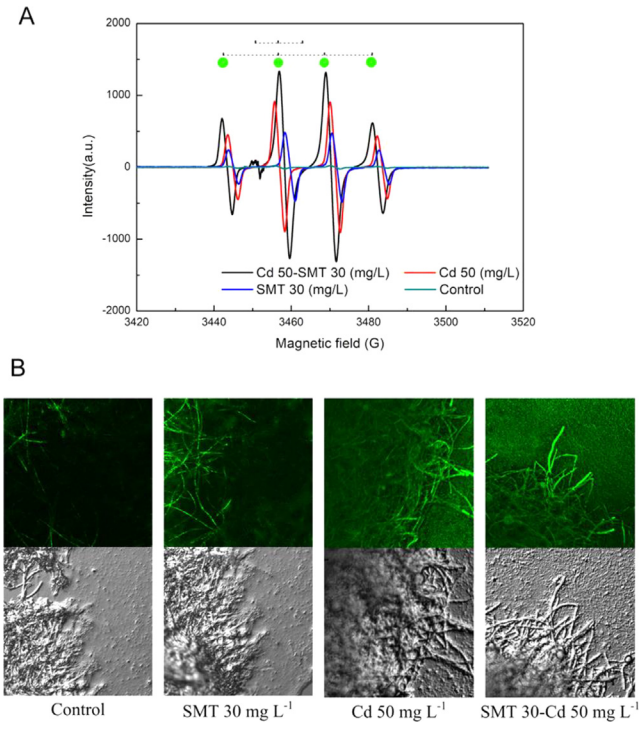

Fig. 2. EPR spectra (A) and confocal laser scanning microscopy images (B) of *P. chrysosporium* induced by 30 mg L^{-1} SMT, 50 mg L^{-1} Cd and Cd 50-SMT 30 mg L^{-1} respectively. The control group was free from xenobiotics stress. Scale bars are 10 μm.

of the superoxide anion into oxygen and hydrogen peroxide [42].

As shown in Fig. 3A, the SOD activities under different xenobiotics stresses were distinctly different with the identical concentrations, and the increase of its activity induced by Cd-SMT combined pollution was obviously higher than other individual pollution. For example, the SOD activities under the stress of Cd 50-SMT 30 mg L^{-1} (46.62 U mg^{-1}) was higher than that under the stress of Cd 50 mg L^{-1} (40.79 U mg^{-1}) and SMT 30 mg L^{-1} (3 5.92 U mg^{-1}) at 48 h, and its activities under the stress of Cd 30-SMT 30 mg L^{-1} (44.17 U mg^{-1}) was higher than that under the stress of Cd 30 mg L^{-1} (38.85 U mg^{-1}) and SMT 30 mg L^{-1}. The activity of SOD in *P. chrysosporium* gradually increased in all samples and the activity of three experimental groups presented a significant increase as compared to the control. After 36 h, the SOD activities of three experimental groups reached the highest level which was 50.47, 44.05 and 38.29 U mg^{-1} respectively. But the control peaked at 48 h with 30.35 U mg^{-1} SOD activities (Fig. 3B). Obviously, the uptrend of SOD activity was consistent with the downtrend of $O_2\cdot^-$ content. That is to say: at the initial time, the concentration of $O_2\cdot^-$ was increased due to xenobiotics exposures, but the SOD activity was stimulated by these stresses and finally scavenged the free radical to alleviate the oxidative damage of cell.

The function of CAT is catalyzing the conversion of hydrogen peroxide to water and oxygen [43]. A low concentration of xenobiotics can also stimulate CAT activities compared to the control, but the CAT activity was inhibited under 100 mg L^{-1} Cd stress (Fig. 3C). At the same concentration, this index induced by SMT was apparently higher than that induced by Cd, and the ration was about 2.15–1.22 at the variation of 30 L^{-1} mg to 50 mg L^{-1}. What is also obvious is that Cd-SMT combined pollution reduced the CAT activity as compared to their individual pollution in every sample of G3. However, data in Fig. 3D display that, before 36 h, the CAT activity under Cd 50-SMT 30 mg L^{-1} stress was higher than that under Cd 50 mg L^{-1} stress. This phenomenon indicated that combined pollution can make *P. chrysosporium* reactive and induce strong stress response at initial time, but toxicity

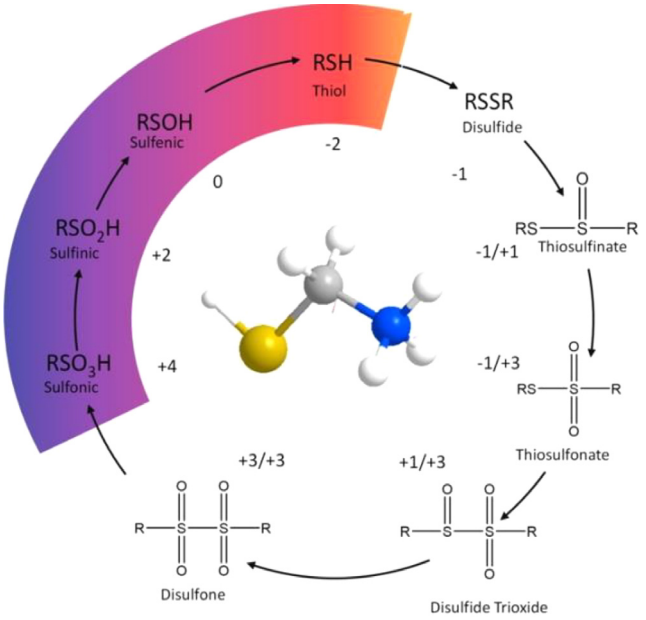

Fig. 4. The existent form and valence of sulfur atoms in sulfhydryl groups referring the biochemical reaction in microorganisms.

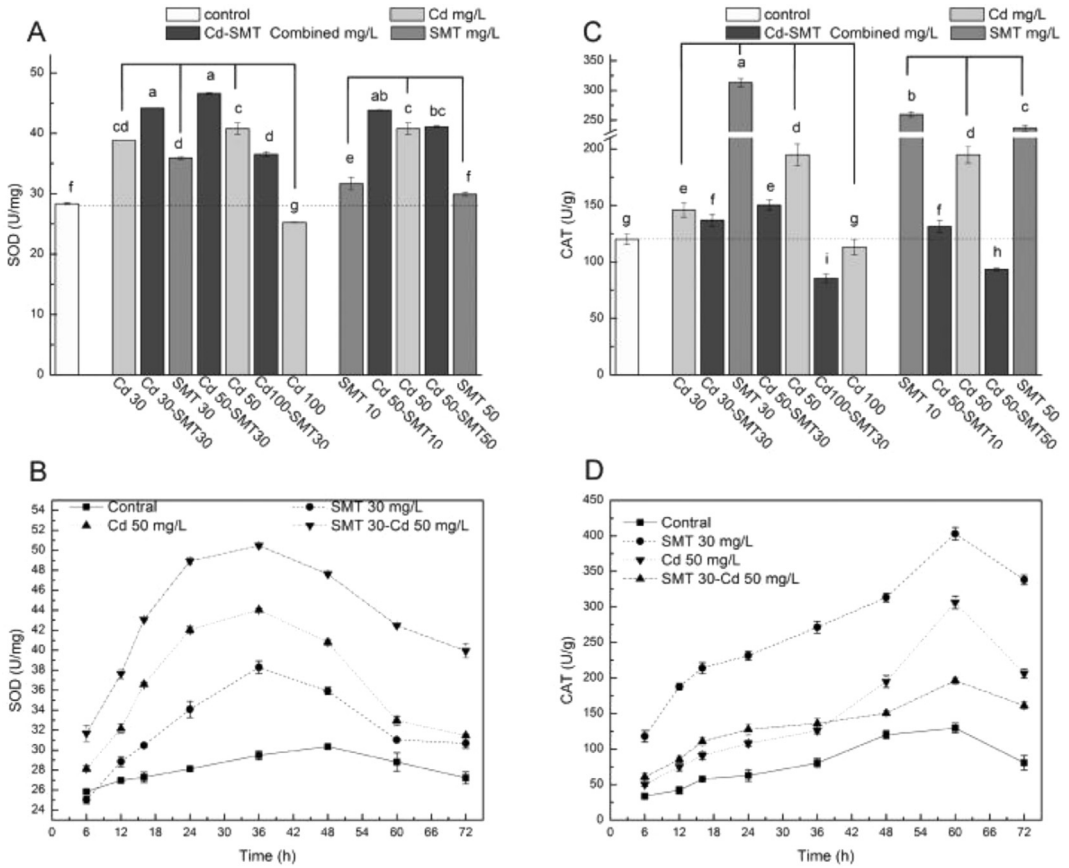

Fig. 3. Concentrations of SOD (A) and CAT (C) exposed to a range of 0–100 mg L^{-1} Cd and 0–50 mg L^{-1} SMT for 48 h, and time-cause of SOD (B) and CAT (D) variation under Cd 50 mg L^{-1}, SMT 30 mg L^{-1} and Cd 50-SMT 30 mg L^{-1} in *P. chrysosporium*. The bars represent the standard deviations of the means (n = 3), and the values followed by different letters in the same figure differ significantly ($p < 0.05$).

increases with time which leads to the decrease of CAT activity. In particular, CAT activity reached a maximum value at 60 h in all samples which was 24 h later than SOD activity. This phenomenon may attribute to the accumulation of hydrogen peroxide, which was produced in SOD catalysis reaction, and can stimulate CAT generation to alleviate hydrogen peroxide-induced oxidative damage.

3.3. Non-enzymatic antioxidants analysis

Thiols which contains carbon-bonded sulfhydryl group are important non-enzymatic antioxidants. They can react with olefin, epikote and many kinds of heavy metals, and play an essential role in intracellular antioxidant system by the conversion of reduction state (R-SH) and oxidation state (RSSR) [44]. They can be oxidized to disulfide, sulfenic, sulfinic and sulfonic. The existent forms and valence of sulfur atoms in sulfhydryl groups referring the biochemical reaction in microorganisms was shown in Fig. 4 [45]. T-SH consists of two main parts: (i) protein thiols (P-SH), manly containing metallothionein, thioredoxin and GSH peroxidase, and (ii) NP-SH, including PCs, GSH, γ-glutathione cysteine and cysteine. In addition to the ROS detoxification, GSH also can react with Cd to form a kind of chelate cadmium-bis-glutathionate (Cd-GS_2) which has two characteristics of structure: (i) thiol groups can react with Cd^{2+} but amino groups cannot; (ii) γ-Glu residue is not related to the formation of metal-hydro sulphonyl chelate [46]. In this study, the concentration of TSH and NP-SH were measured to determine the effect of non-enzymatic antioxidants under Cd-SMT individual and combined stress. In addition, the concentration of P-SH was calculated by subtracting the NP-SH from T-SH concentrations.

As shown in Fig. 5A, the addition of both Cd and SMT to the culture medium led to significant increases in the concentrations of SH compounds. What's more, the higher concentration of xenobiotics, the larger value of both T-SH and NP-SH can be seen to some extent, except for the group under the stress of Cd 100 mgL^{-1} and SMT 50 mg L^{-1}, because too high concentrations of xenobiotics will destroy the regular intracellular resistance system. Furthermore, the levels of SH compounds, induced by Cd-SMT combined pollution, were significantly higher than those of control and individual pollution groups. *P. chrysosporium* grown in medium without any xenobiotics had a T-SH concentration 1.05–1.45 times lower than that of G3, and had a NP-SH concentration 1.56–1.72 times lower than that of G3. The yield of T-SH and NP-SH was significantly affected by exposure time as shown in Fig. 5B. The concentration of SH compounds of control reached the peak value at 12 h (35.50 μmol g^{-1} of T-SH and 11.57 μmol g^{-1} of NP-SH) and the other arrived at the maximum value at 16 h which were higher than the control, then all of them constantly decreased as exposure time went on. The decrease of T-SH from 45.0 to 21.9 μmol g^{-1} under 30 mg L^{-1} SMT was observed from 16 to 72 h. Similarly, the decrease under 50 mg L^{-1} Cd was from 47.0 to 26.2 μmol g^{-1}, and the T-SH under Cd 50-SMT 30 mg L^{-1} was from 49.0 to 27.0 μmol g^{-1}. This phenomenon suggested that: (i) Cd and SMT stimulate the synthesis of thiols in cells especially NP-SH, while the concentration of P-SH relatively have a little change, and (ii) SH compounds may also be involved in Cd-SMT combined and individual detoxification in *P. chrysosporium*. Other researches on GSH induced by HMs in microorganisms also demonstrated that the biosynthetic pathway of GSH can easily affected by HMs exposure and other oxidative stress [47].

3.4. Effects of Cd-SMT stress on cellular damage of P. Chrysosporium

Heavy metals and antibiotic accumulated intracellularly can cause serious damages by thiol-binding and protein denaturation replacing, primary displacement of essential metals involved in biological reactions, or a secondary effect of oxidative stress [48]. MDA is one of the peroxidation products of membrane lipids. Its concentration indicates the peroxidation degree of lipids and the damage degree of cell membrane [49]. According to this study, low concentration of Cd hardly caused the increase of the value of MDA compared with the control treatment in hypha. But the amount of MDA increased as Cd concentration increased: Cd concentration of 100 mg L^{-1} leads the MDA concentration to 0.005 μmol g^{-1} (Fig. 6A). Similar tendency can also be observed for a concentration variation of MDA under SMT stress. However at the same concentration, the MDA value under SMT stress was higher than that under Cd stress, and the ratios of these two trials were around 2.31–1.56 (30–50 mg L^{-1} pollutant). Furthermore, the MDA value of G3 was obviously lower than G1 and G2. From Fig. 6B, the highest MDA content was found at 60 h in all trials except for the control which peaked after 36 h, while a slight decrease occurred at later stage. At the initial time, the MDA content under the stress of Cd was slightly higher than that under the stress of SMT, but the phenomenon was opposite with the gap of growth rate increasing after exposed 16 h. As well the MDA content of G3 still maintained the lowest level among all groups at every point in time.

Protein content is an auxiliary pointer to determine cellular growth behavior and damage of *P. chrysosporium*. Since the absorption of a protein-pigment conjugate at 595 nm varies with protein content over the concentration range 0–1000 μg mL^{-1}, A_{595} was taken as the evaluation standard during this protein analysis experiment [50]. At 48 h, the concentration of protein was the lowest under the condition of

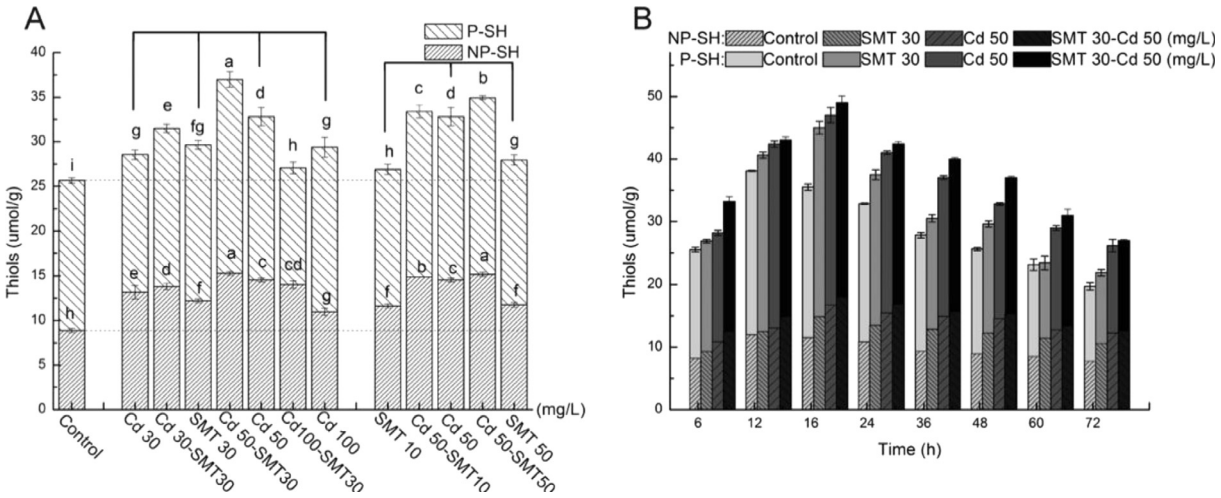

Fig. 5. Concentrations of P-SH and NP-SH (A) exposed to a range of 0–100 mg L^{-1} Cd and 0–50 mg L^{-1} SMT for 48 h, and time-cause of that (B) accumulation under Cd 50 mg L^{-1}, SMT 30 mg L^{-1} and Cd 50-SMT 30 mg L^{-1} in *P. chrysosporium*. The bars represent the standard deviations of the means (n = 3), and the values followed by different letters in the same figure differ significantly ($p < 0.05$).

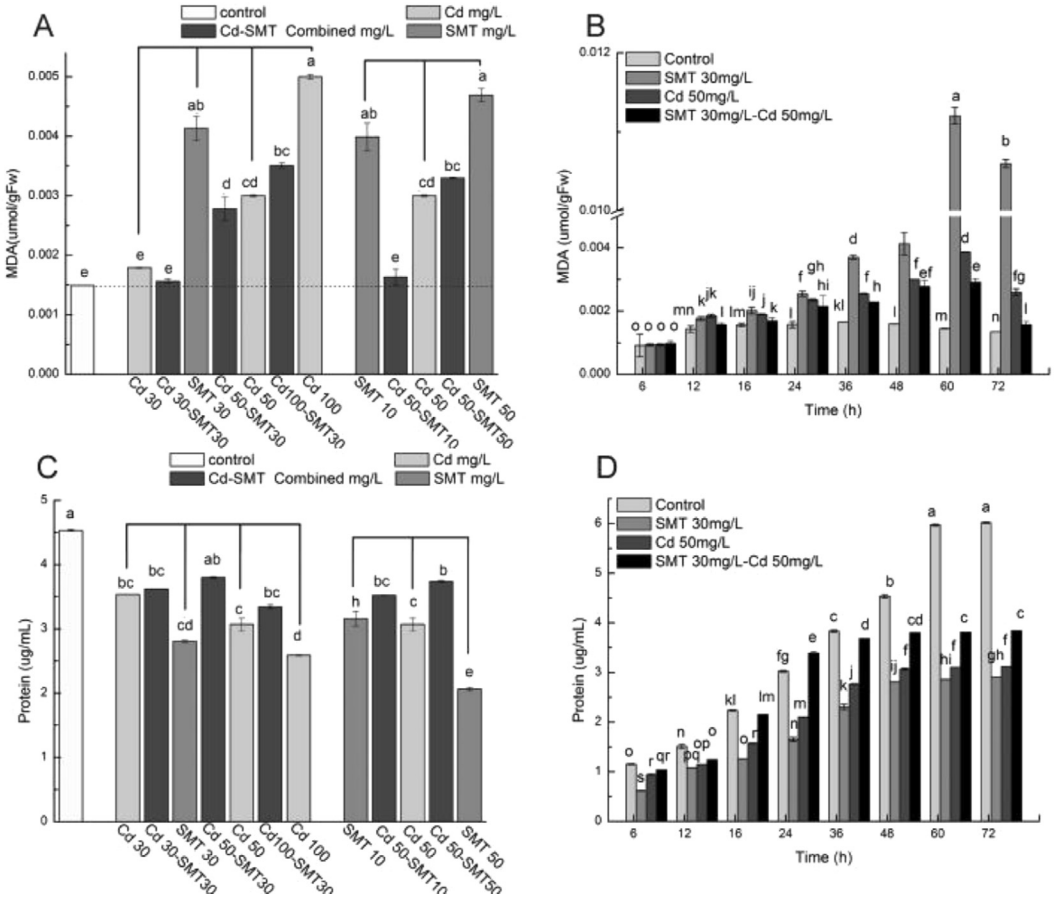

Fig. 6. Concentrations of MDA (A) and protein (C) exposed to a range of 0–100 mg L^{-1} Cd and 0–50 mg L^{-1} SMT for 48 h, and time-cause of MDA (B) and protein (D) accumulation under Cd 50 mg L^{-1}, SMT 30 mg L^{-1} and Cd 50-SMT 30 mg L^{-1} in *P. chrysosporium*. The bars represent the standard deviations of the means (n = 3), and the values followed by different letters in the same figure differ significantly ($p < 0.05$).

50 mg L^{-1} SMT rather than 100 mg L^{-1} Cd (Fig. 6C). With the concentration of SMT increased, protein content decreased in G1, which was similar to the relationship between the concentration of Cd and protein in G2. But in combined pollutant group, the trend was a bit more different. The protein content reached the highest point at Cd 50-SMT 30 mg L^{-1}, which was higher than Cd 50-SMT 10 mg L^{-1} and Cd 30-SMT 30 mg L^{-1} group, potentially due to the bidentate complex way of Cd and SMT [51]. As shown in Fig. 6D, the growth rate of protein in control was revving up before 60 h, while that in experimental groups was conspicuously suppressed after 24 h. Still, the protein content in all group were continuously growing after 72 h. This phenomenon indicated that *P. chrysosporium* can exist under Cd-SMT individual and combined stress. And among three experimental groups, Cd 50-SMT 30 mg L^{-1} was the most suitable and lower toxicity for *P. chrysosporium*. The protein content of each experimental group was lower than the control, owning to two possible reasons: (i) xenobiotics inhibited

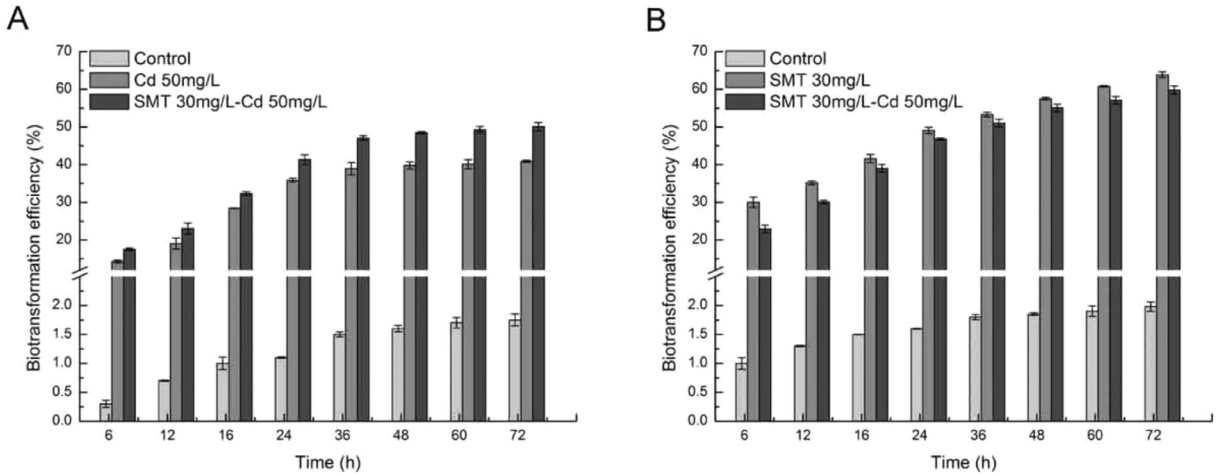

Fig. 7. Time-cause of Cd (A) and SMT (B) biotransformation efficiency under Cd 50 mg L^{-1}, SMT 30 mg L^{-1} and Cd 50-SMT 30 mg L^{-1} in *P. chrysosporium*. The bars represent the standard deviations of the means (n = 3), and the values followed by different letters in the same figure differ significantly ($p < 0.05$).

the growth of *P. chrysosporium*, (ii) protein structure were damaged under the stress of xenobiotics. Proteins are the main targets of free radicals and other oxidants both in extracellular and intracellular reactions. It was estimated that 50–75% free radicals were scavenged by protein among all kinds of macromolecules.

The agents that cause the cellular damage are known as free radicals, which are unpaired molecules. Free radicals are constantly trying to steal electrons from unsaturated fatty acids, which are an important component of cell membrane phospholipids, and associated with cell membrane stability [52]. Then other new free radicals were generated constantly from chain reaction. These free radicals can change the morphology and function of membrane-type proteases, membrane receptors and ionic channel, and finally cause the damage and senescence of fungi cell. Therefore, the cell damage indexes of *P. chrysosporium* growth rose at the beginning then dropped later under the normal conditions, while different kinds of xenobiotics addition aggravated this damage in varying degrees and delayed peak time which potentially related to stimulate the resistance system in fungi cells. These results indicated that the oxidative damage of *P. chrysosporium* membrane lipids by Cd-SMT pollutant was more little than individual pollutant, and the toxicity of *P. chrysosporium* from high to low is: SMT > Cd > Cd-SMT combined. That is to say that *P. chrysosporium* is more adaptable in combined pollutants system and possesses potential to apply in the real environment.

3.5. Biotransformation of SMT-Cd by P. chrysosporium

Cadmium accumulation and SMT biotransformation by *P. chrysosporium* has been reported previously [53,54]. Results in this study showed that *P. chrysosporium* could not only accumulate Cd and biotransform SMT in their individual pollution, but also decrease them in Cd-SMT combined pollution. As shown in Fig. 7A, a linear increase in the biotransformation efficiency of Cd with increasing time at first 36 h was found in *P. chrysosporium*. A slow decrease of Cd biotransformation efficiency was then observed from 48 to 72 h. While the sustainable growth can be observed in SMT biotransformation efficiency before 72 h, which was shown in Fig. 7B. Furthermore, the promotion of Cd removal under the condition of Cd-SMT co-contamination was obvious, but the biotransformation of SMT can be inhibited under the same condition.

The biotransformation efficiency at 48 h by *P. chrysosporium* grown in experimental fluid contaminated with different combinations of Cd and SMT is shown in Table 1. Data displayed that the biotransformation efficiency under the stress of 50 mg L^{-1} (39.80%) was higher than that induced by 30 mg L^{-1} Cd (38.36%), which may due that higher concentrations supplied a kind of important driving force, to overcome the existing mass transfer resistance between heavy metals and biomass, therefore reinforce the active uptake of *P. chrysosporium*. But when the initial concentration of Cd reached a very high level (> 50 mg L^{-1}), the toxicity will inhibit the removal behavior of *P. chrysosporium*. The addition of SMT had a positive impact on Cd removal by *P. chrysosporium*, which presented the phenomenon that the biotransformation efficiency of Cd in G3 was higher than that of G2. When the initial concentration of Cd-SMT co-contamination was 50–50 mg L^{-1}, the biotransformation efficiency of Cd (49.02%) was the highest, and the lowest in G3 was the one under the stress of Cd100-SMT 30 mg L^{-1} (37.51%). The biotransformation efficiency of SMT went down as the concentration increased. But when adding Cd into the initial pollutants with the same amount, the tendency seemed a little different: (i) the addition of Cd had a negative impact on SMT biotransformation by *P. chrysosporium*, which led to that the biotransformation efficiency of SMT in G1 were higher than that of G3, and (ii) the biotransformation efficiency of SMT under the stress of Cd 50-SMT 30 mg L^{-1} (55.07%) was much higher than that induced by Cd 50-SMT 10 mg L^{-1} (35.57%). One possible explanation for that is SMT as a bidentate ligand can complex with heavy metals based on a certain proportion.

Small-molecule transition metal was a kind of wide-used catalysts due to its unstable electronic. The strong catalytic activity transition metals, especially Pd, Au, Pt, Ru and Ag have been widely reported. the Earth-abundant transition metals including Mn, Fe, Co, Ni, Cd and Cu ("biometals") have been comparatively underutilized until the past few years [55]. The addition of Mn^{2+} and Zn^{2+} can promote the hydrolysis of β-lactam antibiotics by metallo β-lactamases effectively catalytic reaction. Because the carbonyl and N atom in β-lactam antibiotics cannot form the conjugated structure, which make it easy to break by electrophile such as metal catalyst [56]. Nanoscale zero-valent iron was an effective activator for Fenton-like removal of SMT. It was mainly responsible for H_2O_2 decomposing to generate radical ·OH for the degradation of SMT [57,58]. But the catalytic effect of Cd^{2+} on the biotransformation of SMT was limited, and no catalytic hydrogenation production detected by the FTIR and magnetic resonance imaging (MRI). The possible reasons were (i) the conjugated structure of SMT make it more stable than β-lactam antibiotics, and (ii) configuration of extra-nuclear electron make the catalytic activity of Cd^{2+} not obvious. Structurally, SMT contains phenylamino group, imino group (NH), and antisymmetric stretching bands sulphone (O═S═O), which could be binding sites for metal ions (Fig. 8) [59]. In the infrared spectra of SMT, the disappearance and significant shift of O═S═O showed that the coordination in the Cd complex involved in O═S═O reaction but with weak response [60]. Measuring chemical shift and relaxation time by MRI is a popular method to determine HMs coordination. Magnetic resonance scans revealed that there was a possible interaction between aniline group and metal ion through sulfonamidic (N15) and pyrimidic (N23) nitrogen atoms (Fig. S2) [61]. What more, in a neutral environment, SMT mainly exists in the form of SMT^0 and SMT^-, so that the covalent bond was the dominant acting force through the N of pyrimidine ring. Additionally in the acid environment, SMT exists mainly in the form of SMT^+ and SMT^0 without electronegative −NH− group. Therefore, as a stronger electron donor of SMT, benzene ring complex with HMs through cation-π interaction.

Summarizing these findings, the removal efficiency of Cd can be prominently increased under the influence of biosorption by *P. chrysosporium* and complexation. Meanwhile a slight fall of the biotransformation efficiency of SMT can be seen in a short-term treatment except for the ratio of Cd and SMT is close to the coordination site amounts of SMT. But Cd-SMT co-contamination can reduce the toxicity of *P. chrysosporium*, which implies an enormous potential of *P. chrysosporium* to biotransform combined pollution for the long term.

4. Conclusions

Tolerance and biotransformation abilities of *P. chrysosporium* for Cd-

Table 1
Effect of Cd-SMT Combined Pollution of *P. chrysosporium*. All the Values are Means of Triplicates ± SD. Different Letters within a Combination of Treatments Indicate Significant Differences (P < 0.05) among Different Treatments.

Treatments		Biotransformation efficiency	
Cd (mg/L)	SMT (mg/L)	Cd (%)	SMT (%)
0	10		62.89 ± 1.19 a
	30		57.54 ± 1.92 b
	50		53.44 ± 2.22 c
30	0	38.36 ± 1.15 c	
	30	42.83 ± 1.67 bc	46.83 ± 0.38 d
50	0	39.80 ± 1.03 c	
	10	42.58 ± 2.19 bc	35.58 ± 0.54 e
	30	48.51 ± 0.52 a	55.07 ± 1.32 bc
	50	49.02 ± 2.42 a	27.65 ± 0.04 g
100	0	30.26 ± 4.41 d	
	30	37.51 ± 0.91 c	32.18 ± 0.64 f

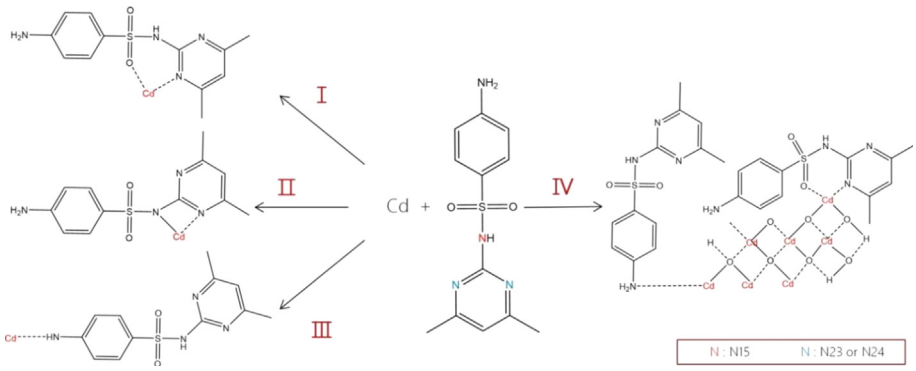

Fig. 8. Possible integrate approaches of Cd and SMT in their Co-contamination.

SMT combined pollutant were obviously enhanced by acclimatization. The concentrations of ROS in hypha were increased under the Cd-SMT individual and combined stress. Excessive concentrations of Cd and SMT caused the oxidative damage of fungi cell, with the increasing of MDA and decreasing of protein. As a response to this phenomenon, the activities of antioxidant enzyme were stimulated as well. Among them, the activity of SOD induced by Cd-SMT co-contamination was higher than that under the stress of their individual pollutant, but the activity of CAT moved in the opposite direction. Non-enzyme antioxidants also play an important role, in which the concentration of NP-SH induced by Cd-SMT co-contamination was higher than that under the stress of their individual pollutant. These stress responses jointly lead to the minor damage of fungi cell and higher biotransformation efficiency of Cd-SMT combined pollutant by *P. chrysosporium* than their individual pollutant. In summary, *P. chrysosporium* bring a promising approach towards biotransformation of Cd-SMT combined pollutant.

Acknowledgments

The present work was financially supported by the Program for the National Natural Science Foundation of China (51579098, 51779090, 51709101, 51278176, 51408206, 51521006), the National Program for Support of Top-Notch Young Professionals of China (2014), Hunan Provincial Science and Technology Plan Project (No.2016RS3026), and the Program for Changjiang Scholars and Innovative Research Team in University (IRT-13R17).

Appendix A. Supplementary data

Supplementary data associated with this article can be found, in the online version, at http://dx.doi.org/10.1016/j.cej.2018.04.089.

References

[1] M. Hvistendahl, China takes aim at rampant antibiotic resistance, Science 336 (2012) 795.
[2] G. Cheng, D. Zeng, C. Huang, Y. Lai, C. Liu, J. Zhang, L. Wan, C. Hu, W. Zhou, Xiong, Efficient degradation of sulfamethazine in simulated and real wastewater at slightly basic pH values using Co-SAM-SCS /H_2O_2 Fenton-like system, Water Res. 138 (2018) 7–18.
[3] D.L. Huang, R.Z. Wang, Y.G. Liu, G.M. Zeng, C. Lai, P. Xu, B.A. Lu, J.J. Xu, C. Wang, C. Huang, Application of molecularly imprinted polymers in wastewater treatment: a review, Environ. Sci. Pollut. Res. Int. 22 (2015) 963–977.
[4] H. Yi, G. Zeng, C. Lai, D. Huang, L. Tang, J. Gong, M. Chen, P. Xu, H. Wang, M. Cheng, C. Zhang, W. Xiong, Environment-friendly fullerene separation methods, Chem. Eng. J. 330 (2017) 134–145.
[5] H.T. Lai, T.S. Wang, C.C. Chou, Implication of light sources and microbial activities on degradation of sulfonamides in water and sediment from a marine shrimp pond, Bioresour. Technol. 102 (2011) 5017–5023.
[6] D. Huang, Y. Wang, C. Zhang, G. Zeng, C. Lai, J. Wan, L. Qin, Y. Zeng, Influence of morphological and chemical features of biochar on hydrogen peroxide activation: implications on sulfamethazine degradation, Rsc Adv. 6 (2016) 73186–73196.
[7] M. Teixidó, J.J. Pignatello, J.L. Beltrán, M. Granados, J. Peccia, Speciation of the ionizable antibiotic sulfamethazine on black carbon (biochar), Environ. Sci. Technol. 45 (2011) 10020–10027.
[8] D. Huang, L. Liu, G. Zeng, P. Xu, H. Chao, L. Deng, R. Wang, W. Jia, The effects of rice straw biochar on indigenous microbial community and enzymes activity in heavy metal-contaminated sediment, Chemosphere 174 (2017) 545–553.
[9] C. Lai, M.M. Wang, G.M. Zeng, Y.G. Liu, D.L. Huang, C. Zhang, R.Z. Wang, P. Xu, M. Cheng, C. Huang, Synthesis of surface molecular imprinted TiO 2 /graphene photocatalyst and its highly efficient photocatalytic degradation of target pollutant under visible light irradiation, Appl. Surf. Sci. 390 (2016) 368–376.
[10] W. Xue, D. Huang, G. Zeng, J. Wan, C. Zhang, R. Xu, M. Cheng, R. Deng, Nanoscale zero-valent iron coated with rhamnolipid as an effective stabilizer for immobilization of Cd and Pb in river sediments, J. Hazard. Mater. 341 (2017) 381–389.
[11] D. Huang, W. Xue, G. Zeng, J. Wan, G. Chen, C. Huang, C. Zhang, M. Cheng, P. Xu, Immobilization of Cd in river sediments by sodium alginate modified nanoscale zero-valent iron: Impact on enzyme activities and microbial community diversity, Water Res. 106 (2016) 15–25.
[12] D. Huang, X. Gong, Y. Liu, G. Zeng, C. Lai, H. Bashir, L. Zhou, D. Wang, P. Xu, M. Cheng, Effects of calcium at toxic concentrations of cadmium in plants, Planta 245 (2017) 863–873.
[13] X. Gong, D. Huang, Y. Liu, G. Zeng, R. Wang, J. Wan, C. Zhang, M. Cheng, X. Qin, W. Xue, Stabilized nanoscale zero-valent iron mediated cadmium accumulation and oxidative damage of Boehmeria nivea (L.) Gaudich cultivated in cadmium contaminated sediments, Environ. Sci. Technol. 51 (2017) 11308–11316.
[14] D. Huang, X. Wang, C. Zhang, G. Zeng, Z. Peng, J. Zhou, M. Cheng, R. Wang, Z. Hu, X. Qin, Sorptive removal of ionizable antibiotic sulfamethazine from aqueous solution by graphene oxide-coated biochar nanocomposites: influencing factors and mechanism, Chemosphere 186 (2017) 414–421.
[15] P. Xu, L. Liu, G. Zeng, D. Huang, C. Lai, M. Zhao, C. Huang, N. Li, Z. Wei, H. Wu, C. Zhang, M. Lai, Y. He, Heavy metal-induced glutathione accumulation and its role in heavy metal detoxification in Phanerochaete chrysosporium, Appl. Microbiol. Biotechnol. 98 (2014) 6409–6418.
[16] D. Huang, C. Hu, G. Zeng, M. Cheng, P. Xu, X. Gong, R. Wang, W. Xue, Combination of Fenton processes and biotreatment for wastewater treatment and soil remediation, Sci. Total Environ. 574 (2017) 1599–1610.
[17] Y.H. Kim, Discovery and characterization of new O-methyltransferase from the genome of the lignin-degrading fungus Phanerochaete chrysosporium for enhanced lignin degradation, Enzyme Microb. Technol. 82 (2016) 66–73.
[18] C.E. Rodríguez-Rodríguez, M.J. García-Galán, P. Blánquez, M.S. Díaz-Cruz, D. Barceló, G. Caminal, T. Vicent, Continuous degradation of a mixture of sulfonamides by Trametes versicolor and identification of metabolites from sulfapyridine and sulfathiazole, J. Hazard. Mater. 213 (2012) 347–354.
[19] X. Li, Y. Wang, Y. Pan, H. Yu, X. Zhang, Y. Shen, S. Jiao, K. Wu, G. La, Y. Yuan, Mechanisms of Cd and Cr removal and tolerance by macrofungus Pleurotus ostreatus HAU-2, J. Hazard. Mater. 330 (2017) 1–8.
[20] M. Naghdi, M. Taheran, S.K. Brar, A. Kermanshahi-Pour, M. Verma, R.Y. Surampalli, Removal of pharmaceutical compounds in water and wastewater using fungal oxidoreductase enzymes, Environ. Pollut. 234 (2017) 190–213.
[21] D. Huang, X. Guo, Z. Peng, G. Zeng, P. Xu, X. Gong, R. Deng, W. Xue, R. Wang, H. Yi, White rot fungi and advanced combined biotechnology with nanomaterials: promising tools for endocrine-disrupting compounds biotransformation, Crit. Rev. Biotechnol. (2017), http://dx.doi.org/10.1080/07388551.2017.1386613.
[22] J.D. Garcia-Garcia, R. Sanchez-Thomas, R. Moreno-Sanchez, Bio-recovery of non-essential heavy metals by intra- and extracellular mechanisms in free-living microorganisms, Biotechnol. Adv. 34 (2016) 859–873.
[23] T.K. Kirk, S. Croan, T. Ming, K.E. Murtagh, R.L. Farrell, Production of multiple ligninases by Phanerochaete chrysosporium: effect of selected growth conditions and use of a mutant strain, Enzyme Microb. Technol. 8 (1986) 27–32.
[24] C. Zhang, C. Lai, G. Zeng, D. Huang, C. Yang, Y. Wang, Y. Zhou, M. Cheng, Efficacy of carbonaceous nanocomposites for sorbing ionizable antibiotic sulfamethazine from aqueous solution, Water Res. 95 (2016) 103–112.
[25] J. Wan, G. Zeng, D. Huang, C. Huang, C. Lai, N. Li, Z. Wei, P. Xu, X. He, M. Lai, Y. He, The oxidative stress of Phanerochaete chrysosporium against lead toxicity, Appl. Biochem. Biotechnol. 175 (2015) 1981–1991.
[26] J.J. Sedmak, S.E. Grossberg, A rapid, sensitive, and versatile assay for protein using Coomassie brilliant blue G250, Anal. Biochem. 79 (1977) 544–552.
[27] W.D. Thomas, Handbook of Methods for Oxygen Radical Research, CRC Press,

1985.
[28] K. Oracz, E.M. Bouteau, J.M. Farrant, K. Cooper, M. Belghazi, C. Job, D. Job, F. Corbineau, C. Bailly, ROS production and protein oxidation as a novel mechanism for seed dormancy alleviation, Plant J. Cell Mol. Biol. 50 (2007) 452–465.
[29] A. Chen, G. Zeng, G. Chen, L. Liu, C. Shang, X. Hu, L. Lu, M. Chen, Y. Zhou, Q. Zhang, Plasma membrane behavior, oxidative damage, and defense mechanism in Phanerochaete chrysosporium under cadmium stress, Process Biochem. 49 (2014) 589–598.
[30] G. Fang, C. Liu, J. Gao, D.D. Dionysiou, D. Zhou, Manipulation of persistent free radicals in biochar to activate persulfate for contaminant degradation, Environ. Sci. Technol. 49 (2015) 5645–5653.
[31] J.F. Robyt, R.J. Ackerman, C.G. Chittenden, Reaction of protein disulfide groups with Ellman's reagent: a case study of the number of sulfhydryl and disulfide groups in Aspergillus oryzae -amylase, papain, and lysozyme, Arch. Biochem. Biophys. 147 (1971) 262–269.
[32] N. Smirnoff, Q.J. Cumbes, Hydroxyl radical scavenging activity of compatible solutes, Phytochemistry 28 (1989) 1057–1060.
[33] L. Liu, P. Xu, G. Zeng, D. Huang, M. Zhao, C. Lai, M. Chen, N. Li, C. Huang, C. Wang, Inherent antioxidant activity and high yield production of antioxidants in Phanerochaete chrysosporium, Biochem. Eng. J. 90 (2014) 245–254.
[34] F.C. Richardforget, M.A. Rouetmayer, P.M. Goupy, J. Philippon, J.J. Nicolas, Oxidation of chlorogenic acid, catechins, and 4-methylcatechol in model solutions by apple polyphenol oxidase, J. Agric. Food Chem. 40 (1992) 2114–2122.
[35] S.J. Stohs, D. Bagchi, Oxidative mechanisms in the toxicity of metal ions, Free Radic. Biol. Med. 18 (1995) 321–336.
[36] D. Huang, X. Qin, P. Xu, G. Zeng, Z. Peng, R. Wang, J. Wan, X. Gong, W. Xue, Composting of 4-nonylphenol-contaminated river sediment with inocula of Phanerochaete chrysosporium, Bioresour. Technol. 221 (2016) 47–54.
[37] M. Cheng, G. Zeng, D. Huang, L. Liu, M. Zhao, C. Lai, C. Huang, Z. Wei, N. Li, P. Xu, Effect of Pb^{2+} on the production of hydroxyl radical during solid-state fermentation of straw with Phanerochaete chrysosporium, Biochem. Eng. J. 84 (2014) 9–15.
[38] M. Cheng, G. Zeng, D. Huang, C. Lai, P. Xu, C. Zhang, Y. Liu, J. Wan, X. Gong, Y. Zhu, Degradation of atrazine by a novel Fenton-like process and assessment the influence on the treated soil, J. Hazard. Mater. 312 (2016) 184–191.
[39] M. Cheng, G. Zeng, D. Huang, L. Cui, P. Xu, C. Zhang, Y. Liu, Hydroxyl radicals based advanced oxidation processes (AOPs) for remediation of soils contaminated with organic compounds: a review, Chem. Eng. J. 284 (2016) 582–598.
[40] L.J. Forney, C.A. Reddy, M. Tien, S.D. Aust, The involvement of hydroxyl radical derived from hydrogen peroxide in lignin degradation by the white rot fungus Phanerochaete chrysosporium, J. Biol. Chem. 257 (1982) 11455–11462.
[41] Z. Han, J. Guo, W. Li, $Fe(bpy)_3^{2+}$ supported on amidoximated PAN fiber as effective catalyst for the photodegradation of organic dye under visible light irradiation, Chem. Eng. J. 228 (2013) 36–44.
[42] M. Castro-Alférez, M.I. Polo-López, J. Marugán, F.I. Pilar, Mechanistic model of the Escherichia coli, inactivation by solar disinfection based on the photo-generation of internal ROS and the photo-inactivation of enzymes: CAT and SOD, Chem. Eng. J. 318 (2016) 214–223.
[43] P.R.F. Rosa, B.C. Gomes, M.B.A. Varesche, E.L. Silva, Characterization and antimicrobial activity of lactic acid bacteria from fermentative bioreactors during hydrogen production using cassava processing wastewater, Chem. Eng. J. 284 (2016) 1–9.
[44] N. Patsoukis, C.D. Georgiou, Determination of the thiol redox state of organisms: new oxidative stress indicators, Anal. Bioanal. Chem. 378 (2004) 1783–1792.
[45] K.G. Reddie, K.S. Carroll, Expanding the functional diversity of proteins through cysteine oxidation, Curr. Opin. Chem. Biol. 12 (2008) 746–754.
[46] O. Delalande, H. Desvaux, E. Godat, A. Valleix, C. Junot, J. Labarre, Y. Boulard, Cadmium-glutathione solution structures provide new insights into heavy metal detoxification, FEBS J. 277 (2010) 5086–5096.
[47] L. Zhang, H. Li, X. Lai, X. Su, T. Liang, Thiola X.R. Zeng, Ted graphene-based superhydrophobic sponges for oil-water separation, Chem. Eng. J. 316 (2017) 736–1734.
[48] E. Fourest, J.C. Roux, Heavy metal biosorption by fungal mycelial by-products: mechanisms and influence of pH, Appl. Microbiol. Biotechnol. 37 (1992) 399–403.
[49] L. Wang, C. Zhang, F. Gao, G. Mailhot, G. P, Algae decorated TiO2 /Ag hybrid nanofiber membrane with enhanced photocatalytic activity for Cr (VI) removal under visible light, Chem. Eng. J. 314 (2017) 622–630.
[50] Y. Du, X. Tao, K. Shi, Y. Li, Degradation of lignite model compounds by the action of white rot fungi, Min. Sci. Technol. (China) 20 (2010) 76–81.
[51] A.M. Mansour, Experimental and quantum chemical studies of sulfamethazine complexes with Ni(II) and Cu(II) ions, J. Coord. Chem. 66 (2013) 1118–1128.
[52] C. Huang, C. Lai, P. Xu, G. Zeng, D. Huang, J. Zhang, C. Zhang, M. Cheng, J. Wan, R. Wang, Lead-induced oxidative stress and antioxidant response provide insight into the tolerance of Phanerochaete chrysosporium to lead exposure, Chemosphere 187 (2017) 70–77.
[53] P. Xu, Y. Leng, G. Zeng, D. Huang, C. Lai, M. Zhao, Z. Wei, N. Li, C. Huang, C. Zhang, Cadmium induced oxalic acid secretion and its role in metal uptake and detoxification mechanisms in Phanerochaete chrysosporium, Appl. Microbiol. Biotechnol. 99 (2015) 435–443.
[54] A. Prieto, M. Möder, R. Rodil, L. Adrian, E. Marco-Urrea, Degradation of the antibiotics norfloxacin and ciprofloxacin by a white-rot fungus and identification of degradation products, Bioresour. Technol. 102 (2011) 10987–10995.
[55] D. Wang, D. Astruc, The recent development of efficient Earth-abundant transition-metal nanocatalysts, Chem. Soc. Rev. 46 (2017) 816–854.
[56] H. Chen, Y.F. Shi, Study on essential residues of VIM metal-β-lactamases for bacteria resistance to carbapenems, J. Dalian Polytech. Univ. 31 (2012) 172–176.
[57] J. Deng, H. Dong, C. Zhang, Z. Jiang, Y. Cheng, K. Hou, L. Zhang, C. Fan, Nanoscale zero-valent iron/biochar composite as an activator for Fenton-like removal of sulfamethazine, Sep. Purif. Technol. 202 (2018) 130–137.
[58] M. Stefaniuk, P. Oleszczuk, S.O. Yong, Review on nano zerovalent iron (nZVI): from synthesis to environmental applications, Chem. Eng. J. 287 (2016) 618–632.
[59] B. Kesimli, A. Topacli, Infrared studies on Co and Cd complexes of sulfamethoxazole, Spectrochim. Acta A. 57 (2001) 1031–1036.
[60] A.M. Mansour, Molecular structure and spectroscopic properties of novel manganese(II) complex with sulfamethazine drug, J. Mol. Struct. 1035 (2013) 114–123.
[61] X. Qu, P. Liu, D. Zhu, Enhanced sorption of polycyclic aromatic hydrocarbons to Tetra-Alkyl ammonium modified smectites via cation − π interactions, Environ. Sci. Technol. 42 (2008) 1109–1116.